

CORROSION AND ELECTROCHEMICAL PROPERTIES OF Sn/Mg-MODIFIED ALUMINUM ALLOYS AFTER HEAT TREATMENT FOR METAL-AIR BATTERIES

KOROZIJA IN ELEKTROKEMIJSKE LASTNOSTI S KOSITROM IN MAGNEZIJEM MODIFICIRANE ALUMINIJEVE ZLITINE PO TOPLLOTNI OBELAVI ZA KOVINSKO-ZRAČNE BATERIJE

Na Xu*, Di Wang, Zhiqiang Xu

Liaodong University, 116 Linjiang Back Street, Dandong, 118001, P. R. China

Prejem rokopisa – received: 2025-10-07; sprejem za objavo – accepted for publication: 2026-1-09

doi:10.17222/mit.2025.1585

This study systematically investigates the effects of Sn, Mg and heat treatment on the electrochemical performance and corrosion resistance of aluminum alloys in metal-air batteries. A series of alloy samples were prepared by melting, including pure aluminum, alloys with varying Sn content (0.5, 1.5, 2.5) wt %, and corresponding alloys with 5 wt % Mg addition. Electrochemical impedance spectroscopy and polarization curves were tested in 0.1 mol/L NaOH solution. The results indicate that Sn reduces the corrosion resistance of alloys under non-deformed and low-deformation conditions, while it helps to increase the impedance under high-deformation conditions. The addition of Mg significantly enhances the stability of the passive film, exhibiting higher impedance under all conditions. The synergistic effect of Sn and Mg effectively improves the electrochemical performance of the alloys. This research reveals the significant influence of Sn-Mg dual-element synergy on the electrochemical behavior of aluminum alloys, clarifies the crucial role of Mg in enhancing corrosion resistance, and provides a theoretical foundation and practical reference for the design of high-performance anodes for aluminum-air batteries.

Keywords: tin-modified aluminum alloy, heat treatment, electrochemical impedance spectroscopy, magnesium, corrosion resistance

Avtorji v tem članku opisujejo študijo sistematične raziskave vpliva kositra (Sn) in magnezija (Mg) ter toplotne obdelave na elektro-kemijske lastnosti in korozijsko odpornost aluminijevih zlitin namenjenih za izdelavo anod kovinsko zračnih baterij (angl.: metal-air batteries). Avtorji so pripravili serijo Al zlitin z različno vsebnostjo Sn (0,5, 1,5, 2,5 wt%) in še eno serijo teh zlitin z dodatkom 5 wt% Mg. Raztaljeni tehnično čisti Al (>99,9 %) so legirali z izbranimi vsebnostmi Sn in Mg. Sledila je elektro-kemijska impedančna spektroskopija zlitin v 0,1 mol/L raztopini natrijevega luga (NaOH). Rezultati analiz so pokazali, da Sn zmanjšuje korozijsko odpornost zlitin v nedeformiranem in malo deformiranem stanju, medtem ko povečuje impedanco zlitin v močno deformiranem stanju. Dodatek Mg močno izboljša stabilnost formiranega pasivnega filma, kar zviša impedanco zlitin v vseh stanjih. Sinergistični učinek legiranja Al s Sn in Mg učinkovito izboljša elektro-kemijske performanse zlitin. S to raziskavo so avtorji odkrili pomemben sinergijski vpliv dvojnega legiranja s Sn in Mg na elektro-kemijsko obnašanje aluminijevih zlitin in pojasnjuje ključno vlogo Mg pri izboljšanju njihove korozijske odpornosti, kar zagotavlja teoretične temelje in praktične reference oblikovanja (dizajna) visoko kakovostnih anod za kovinsko zračne baterije.

Ključne besede: s kositrom in magnezijem modificirane Al zlitine, toplotna obdelava, elektro-kemijska impedančna spektroskopija, magnezij, korozijska odpornost.

1 INTRODUCTION

In recent years, with the rapid growth in demand for green energy and efficient energy storage, aluminum-air batteries have garnered significant attention due to their combination of aluminum's high theoretical specific capacity and the core advantages of open-system oxygen-reduction reactions. These batteries offer high theoretical energy density (up to 800–1200 Wh/kg), environmental friendliness, and resource sustainability (the aluminum recycling rate exceeds 95 %). However, in aluminum-air batteries, which use metallic aluminum

as the anode and oxygen from the air as the cathode active material, the surface oxide film of aluminum alloys in alkaline electrolytes such as NaOH or KOH struggles to withstand high-concentration corrosive media. Coupled with the high reactivity of aluminum, this leads to severe corrosion, significant material loss, and reduced service life. As a result, anode utilization remains low (typically below 40 %), and battery performance degrades considerably, severely limiting any practical application.

Tin (Sn) serves as an efficient activating element, disrupting the passive film on aluminum alloys through micro-galvanic effects and dissolution-deposition synergy. However, the introduction of Sn can also induce localized corrosion, reducing the overall corrosion resistance of the material. When the Sn content exceeds the solid-solubility limit, precipitated Sn-rich phases form

*Corresponding author's e-mail:
manmanhappytu@126.com (Na Xu)



© 2026 The Author(s). Except when otherwise noted, articles in this journal are published under the terms and conditions of the Creative Commons Attribution 4.0 International License (CC BY 4.0).

micro-galvanic couples with the aluminum matrix, with a potential difference of approximately 1 V. This triggers the preferential dissolution of aluminum and damages the passive film, while Sn-rich phases catalyze hydrogen evolution and establish a self-corrosion cycle. Sn⁴⁺ ions (0.069 nm radius) intrude into the Al₂O₃ lattice, causing distortion and significantly increasing the defect density. This reduces the oxide film resistance from 10¹⁴ Ω·cm to 10⁶–10⁸ Ω·cm and markedly lowers the charge-transfer resistance. Meanwhile, the conduction band of SnO₂ (–0.3 V) is closer to the hydrogen evolution potential (–0.83 V) than that of Al₂O₃ (–1.5 V), creating an energy gradient that promotes electron leakage. Sn dissolved in an alkaline solution can redeposit as nano-sized SnO₂ particles. In the eutectic structure of aluminum-tin alloys, the aluminum-rich matrix provides strength and conductivity, while dispersed Sn phases act as solid lubricants.

To balance the "high activity" and "high corrosion resistance" of aluminum-air battery anodes, a combined strategy of multi-element alloying and process optimization has become mainstream. Researchers at RWTH Aachen University in Germany confirmed that Sn-Mg atomic pairs exhibit a binding energy of –3.2 eV, effectively suppressing hydrogen evolution, though the alloys are sensitive to electrolyte fluctuations. MIT introduced La to purify the grain boundaries and improve the electrolyte adaptability, but this increases costs. The Harbin Institute of Technology utilized electromagnetic oscillation to refine the microstructure and reduce corrosion rates, albeit with higher energy consumption. The Korea Institute of Materials Science applied plasma electrolytic oxidation (PEO) to form a porous ceramic layer that enhances oxygen diffusion, but at the cost of increased interfacial resistance. In aluminum-air battery systems, the synergistic interaction between magnesium (Mg) and tin (Sn) plays a critical role in improving the electrochemical behavior of alloys. Studies have shown that in alkaline media (e.g., 0.1–4 mol/L NaOH), controlling the Sn content (typically 0.5–2.5 w%) and introducing elements such as Mg can significantly enhance the electrochemical performance of the alloy. The addition of Mg exhibits a dual effect: on one hand, it forms compounds with impurity elements (such as Mg(OH)₂ or MgAl₂O₄ spinel structures), enhancing the stability of the passive film, reducing cathodic phases by over 40 %, and effectively suppressing the hydrogen-evolution reaction; on the other hand, its low potential characteristics contribute to the formation of a dynamic passive film, significantly increasing the hydrogen-evolution overpotential and reducing the hydrogen evolution current. Furthermore, Mg refines the grain structure to the submicron level, increases micro-galvanic couple density by approximately 40 %, expands the reaction interface, and promotes uniform corrosion. Sn effectively disrupts the passive film of aluminum alloys through a multi-scale synergistic mechanism, spanning from atomic substitution to mi-

cro-phase distribution, and works in concert with dynamic deposition and multi-element activation processes to form an efficient activation network. The synergistic effect of Mg and Sn forms an efficient activation network at 0.03 w% Sn, effectively overcoming passivation and demonstrating a strong potential for industrialization.

Studies have shown that Mg can significantly reduce the area of detrimental cathodic phases in aluminum alloys, either through the formation of Mg₂Si and other phases or by altering precipitation behavior.² It has been reported that the reduction can reach over 40 %.² Furthermore, the addition of Mg is believed to refine the microstructure and increase the density of micro-galvanic couples during corrosion.³ However, the manifestation of these effects in Al–Sn-based alloy systems, particularly under alkaline conditions, remains unclear. This study aims to investigate how the introduction of Mg interacts with Sn and influences the electrochemical behavior of the alloy under the aforementioned conditions.

The Mg-Sn synergistic approach reduces material costs by 98 % and increases the casting fluidity index to 120 cm. It achieves an anode utilization rate of 91 %, nearly 60 % higher than that of pure aluminum, breaking through the limitations of single-element modification. This provides a low-cost, high-efficiency solution for highly active aluminum-air battery anodes, advancing their commercialization. Heat treatment is a key process for regulating the microstructure and properties of aluminum alloys. Through processes such as solution treatment, aging, and annealing, the distribution of Sn can be optimized, grain boundary segregation reduced, and the uniform precipitation of secondary phases (e.g., Mg₂Sn) promoted, thereby significantly enhancing the corrosion resistance of the alloy. This study focuses on the influence of heat treatment on the electrochemical performance of Al-Sn alloys, aiming to improve the corrosion resistance and electrochemical stability of aluminum-air battery anodes. It emphasizes the optimization of preparation processes and performance-regulation mechanisms of Sn- and Mg-synergistically modified aluminum alloys.

According to the Al–Sn binary alloy phase diagram, the solid solubility of Sn in Al increases significantly with temperature, reaching a maximum equilibrium solubility of approximately 2.2 w% at temperatures around 490–500 °C below the eutectic temperature (≈655 °C).⁴ Therefore, conducting a solution treatment within this temperature range is expected to maximize the dissolution of Sn (≤2.5 w%).

The study systematically investigates the effects of different solution temperatures on the open-circuit potential, polarization behavior, and impedance characteristics of Al-Sn alloys. By establishing the relationship among "composition–heat treatment–microstructure–electrochemical performance," the synergistic enhancement effect of Sn and Mg is clarified, to further optimize the corrosion resistance of Al-Sn alloys. This provides a

solid theoretical foundation and feasible process pathways for the development of high-performance anode materials for aluminum-air batteries. Additionally, suitable combined heat-treatment processes can further optimize the surface-passivation behavior through grain refinement and dislocation regulation, significantly improving the electrochemical stability of the alloy in alkaline environments.

2 EXPERIMENTAL PRINCIPLES AND METHODS

This experiment employed industrial-grade, high-purity aluminum ingots ($\text{Al} \geq 99.9 \text{ w}\%$), supplemented with pure tin particles ($\text{Sn} \geq 99.9 \text{ w}\%$, particle size 0.5–1 mm) and pure magnesium blocks ($\text{Mg} \geq 99.9 \text{ w}\%$). The tin particles were vacuum-sealed for storage to ensure the SnO_2 content remained $\leq 0.05 \text{ w}\%$, while the magnesium blocks were pickled with 5 % HNO_3 for 30 s and stored in an environment with humidity $\leq 10 \text{ \% RH}$.

All alloys were melted in an SX2-12-16 chamber resistance furnace, with the temperature precisely controlled at $760 \text{ }^\circ\text{C} \pm 2 \text{ }^\circ\text{C}$ under argon protection (flow rate: 5 L/min), using an 8 L high-purity graphite crucible. The aluminum ingots were first melted at $750 \text{ }^\circ\text{C} \pm 5 \text{ }^\circ\text{C}$, after which tin particles and magnesium blocks were added sequentially according to the designed proportions. For Al-xSn-5Mg alloys, a three-stage gradient magnesium addition method was applied at 5-minute intervals, accompanied by a $\text{K}_2\text{TiF}_6\text{-KCl}$ covering agent (mass ratio 1:3, purity $\geq 99.5 \text{ \%}$) to control the magnesium burn-off rate within $2.3 \text{ \%} \pm 0.2 \text{ \%}$. The melt was stirred at 200 min^{-1} for 30 min for homogenization, followed by the addition of 0.1 w% hexachloroethane for refining, ensuring the inclusion content did not exceed 0.03 %. The melt was then poured into a 250°C preheated H13 steel mold and air-cooled at 15°C/s to obtain the ingot. Alloy composition was verified by spectrometry, with deviations controlled within $\text{Sn} \pm 0.03 \text{ w}\%$ and $\text{Mg} \pm 0.15 \text{ w}\%$. Annealing was performed in a GSL-1600X tube furnace with a temperature control accuracy of $\pm 1 \text{ }^\circ\text{C}$, under a high-purity nitrogen atmosphere (flow rate: 10 L/min, dew point $\leq -60 \text{ }^\circ\text{C}$).

A total of eight sample groups were designed. The ingots were wire-cut into $20 \text{ mm} \times 20 \text{ mm} \times 2 \text{ mm}$ initial samples, each divided into four parallel specimens (32

pieces in total) for solution heat treatment and control experiments, ultimately processed into standard thin sheets of $0.8 \text{ mm} \times 0.8 \text{ mm} \times 1 \text{ mm}$. Specific parameters are listed in **Table 1**.

Material pretreatment included mechanical milling of the aluminum ingot surface to remove a 0.5-mm-thick oxide layer and chemical degreasing (using 10 % NaOH solution at 60°C for 5 min). This was followed by rinsing with deionized water until conductivity dropped to $\leq 2 \text{ }\mu\text{S/cm}$. Each group of ingots was cut into four parallel specimens, processed as follows: three specimens underwent solution treatment at $480 \text{ }^\circ\text{C}$, $490 \text{ }^\circ\text{C}$, and $500 \text{ }^\circ\text{C}$, respectively, in a tube annealing furnace, held for $50 \pm 2 \text{ min}$ followed by water quenching (using $25 \pm 2 \text{ }^\circ\text{C}$ deionized water); the remaining one served as the untreated control group.

All specimens were wire-cut into $0.8 \text{ mm} \times 0.8 \text{ mm} \times 1 \text{ mm}$ sheets, followed by vacuum annealing at $200 \text{ }^\circ\text{C}$ for 1 h to relieve stress. Subsequently, the samples were mechanically polished sequentially with diamond pastes of different grit sizes (9 μm , 3 μm , 1 μm), and were finally fine-polished using a 0.05- μm alumina suspension. After rinsing with deionized water, brief etching in a 10 % HCl solution to remove the oxide layer, and ultrasonic cleaning in ethanol, a contact surface profilometer was employed to verify the surface roughness at multiple random locations. The standardized polishing procedure described above ensured that the initial surface roughness of all the tested samples reached $R_a \leq 0.1 \text{ }\mu\text{m}$. This procedure, validated in our group's previous work and similar electrochemical studies, consistently yields stable and reproducible test surfaces with a final roughness of $R_a \leq 0.1 \text{ }\mu\text{m}$.

Random inspection of 10 % of the specimens showed that the Mg_2Sn phase in the Al-2.5Sn-5Mg alloy had an average size of $1.2 \pm 0.3 \text{ }\mu\text{m}$ and a distribution uniformity index of 0.89, meeting process standards. A 0.1 mol/L NaOH solution was used as the base electrolyte, prepared as follows: first, analytical pure NaOH was dissolved in deionized water and stirred at 600 min^{-1} for 1.5 h until fully dissolved. The solution was then left to stand for 12 h, the electrolyte solution was filtered through a 0.22 μm polytetrafluoroethylene (or nylon) microporous membrane to remove trace insoluble carbonate particles and microorganisms.⁵ This step eliminates solid particles or colloidal contaminants potentially introduced during solution preparation and transfer,

Table 1: Experimental groups and parameters

Alloy System	Sn Content (w%)	Mg Content (w%)	Heat Treatment Temperature ($^\circ\text{C}$)	Note / Group Designation
Al-Sn	0.5	–	480, 490, 500, as-cast	Variables: Sn content, temperature
	1.5	–	480, 490, 500, as-cast	
	2.5	–	480, 490, 500, as-cast	
Al-Sn-5Mg	0.5	5.0	480, 490, 500, as-cast	Variables: Sn content, temperature, Mg addition
	1.5	5.0	480, 490, 500, as-cast	
	2.5	5.0	480, 490, 500, as-cast	

thereby ensuring the physical cleanliness of the electrolyte and preventing the adsorption or deposition of such particles on the electrode surface, which could otherwise interfere with the stability and reproducibility of electrochemical measurements.

The solution pH was calibrated to 12.6 ± 0.1 using a pH meter. This low-concentration electrolyte system effectively reduced the localized corrosion tendency of the aluminum anode. Tafel test results showed that the self-corrosion current density significantly decreased from 1.2 mA/cm^2 in 4 mol/L NaOH to 0.38 mA/cm^2 . However, the decrease in ionic conductivity necessitates compensation through optimized alloy composition.

3 EFFECT OF HEAT TREATMENT PROCESS ON THE ELECTROCHEMICAL PERFORMANCE OF Al-Sn ALLOYS

Open-circuit potential (OCP) serves as a critical indicator for evaluating the electrochemical stability of material surfaces. Its variations directly reflect the integrity of the passive film, corrosion driving force, and distribution of surface active sites.

Analysis of the open-circuit potential of Al-Sn alloys subjected to different heat treatment temperatures (**Figure 1**) reveals that the Al-1.5Sn alloy solution-treated at $490 \text{ }^\circ\text{C}$ exhibits a potential fluctuation amplitude of less than 10 mV during the 3-minute test, indicating a relatively high degree of electrochemical stability at its sur-

face. This enhanced stability is primarily attributed to the uniform dissolution of Sn promoted by the heat treatment, which reduces Sn segregation at grain boundaries and thereby facilitates the formation of a continuous and dense Al_2O_3 -based passive film. This film effectively homogenizes surface electrochemical activity and suppresses the initiation of localized corrosion.

This stability primarily stems from the heat treatment promoting the uniform dissolution of Sn (at $490 \text{ }^\circ\text{C}$, the solid solubility of Sn approaches its maximum value of $2.2 \text{ w}\%$), which reduces Sn segregation at grain boundaries and consequently facilitates the formation of a continuous and dense Al_2O_3 -SnO₂ composite passive film. This composite film effectively mitigates the heterogeneity in surface electrochemical activity, thereby suppressing the initiation of localized corrosion.

In contrast, alloys with a high Sn content (e.g., Al-2.5Sn) demonstrate abnormal OCP fluctuations. This phenomenon can be attributed to the micro-galvanic effect caused by excessive Sn accumulation at grain boundaries, leading to localized preferential dissolution and accelerated negative potential shift. Furthermore, high Sn content promotes the adsorption of surface hydroxyl groups, further exacerbating the anodic dissolution reaction of the aluminum matrix.

Analysis of the polarization curves for Al-Sn alloys after heat treatment, as shown in **Figure 2** reveals significant differences in polarization behavior among alloys with varying Sn contents. Following heat treatment at

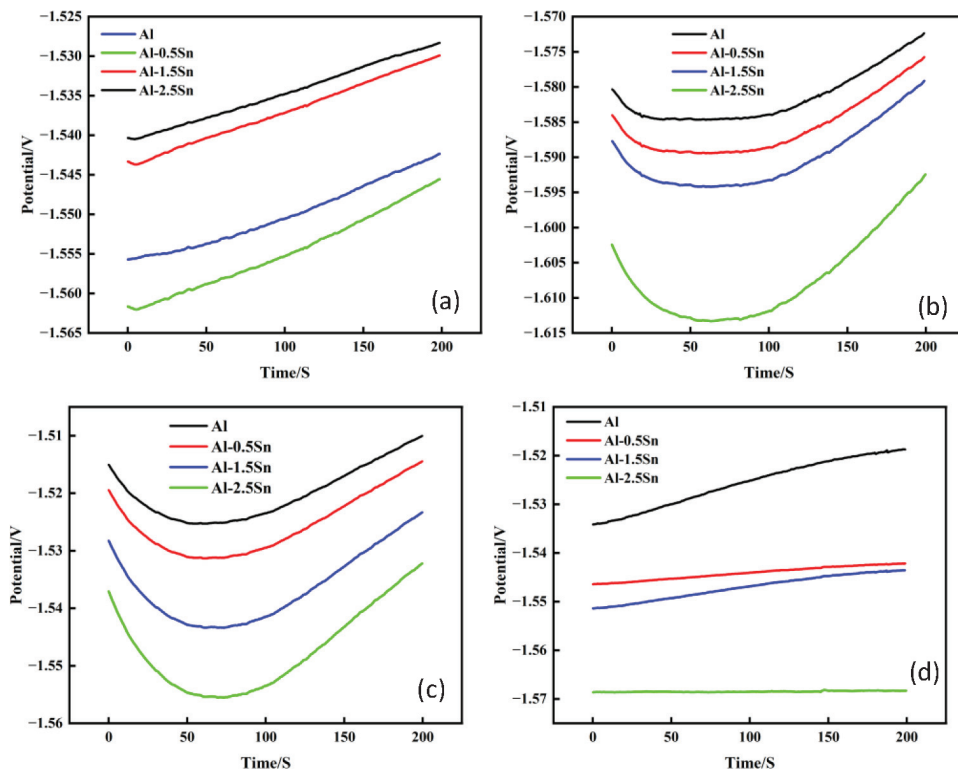


Figure 1: Open-circuit potential (OCP) of Al-Sn alloys under different heat treatment temperatures: a) $480 \text{ }^\circ\text{C}$, b) $490 \text{ }^\circ\text{C}$, c) $500 \text{ }^\circ\text{C}$, and d) control group

480 °C, the self-corrosion potential of the alloys gradually shifts in the negative direction with increasing Sn content, accompanied by a slight rise in corrosion current density. This indicates that the addition of Sn reduces the corrosion resistance of the alloys to some extent. Notably, the alloy with 2.5 % Sn exhibits the highest corrosion current density, demonstrating the poorest corrosion resistance in NaOH solution. When the heat treatment temperature is increased to 490 °C, the self-corrosion potential of the samples shifts positively compared to those treated at 480 °C. Moreover, the corrosion current density shows varying trends with increasing Sn content. At this temperature, the alloy with 1.5 % Sn displays the lowest corrosion current, indicating optimal corrosion resistance. After heat treatment at 500 °C, the overall corrosion resistance of the alloys improves significantly. Specifically, the corrosion current of the 0.5Sn and 1.5Sn alloys decreases markedly. However, the 2.5Sn alloy still maintains a relatively high corrosion current density, suggesting that excessive Sn content cannot be effectively mitigated at this temperature to improve corrosion resistance. In contrast, the untreated samples exhibit the lowest self-corrosion potential and the highest corrosion current density, indicating the poorest corrosion resistance. This is likely attributed to the uneven distribution of Sn and Al in the as-cast alloy, which promotes the formation of micro-galvanic cells and accelerates the corrosion process. In summary, heat treatment temperature significantly influences the corrosion resistance of Sn-modified aluminum alloys. Sam-

ples treated at 490 °C and 500 °C generally exhibit superior corrosion resistance, with the 1.5Sn alloy demonstrating particularly outstanding performance. By selecting an appropriate heat treatment temperature, the microstructure of the alloy can be optimized, thereby effectively enhancing the corrosion resistance of Sn-modified aluminum alloys in alkaline environments.

Figure 3 presents the electrochemical impedance spectra of Al-Sn alloys after heat treatment at different temperatures. For the non-heat-treated samples, the Sn content significantly influences their impedance behavior. The pure aluminum sample exhibits the highest impedance, characterized by a large capacitive arc in the Nyquist plot, indicating high charge transfer resistance, low corrosion current density, and superior corrosion resistance. As the Sn content increases, the impedance of the alloys gradually decreases, suggesting that the introduction of Sn compromises their corrosion resistance. The sample with the highest Sn content shows the lowest impedance, which may be attributed to the uneven distribution of Sn in the aluminum matrix, leading to the formation of localized corrosion zones and an accelerated charge-transfer process. After heat treatment at 480 °C, pure aluminum maintains the highest impedance with no significant change in electrochemical stability. However, the impedance of the alloys gradually decreases with increasing Sn content, with the Al-2.5Sn sample exhibiting the lowest impedance. At this temperature, Sn is not fully dissolved in the aluminum matrix, forming microscopic precipitates that increase electrochemical activity.

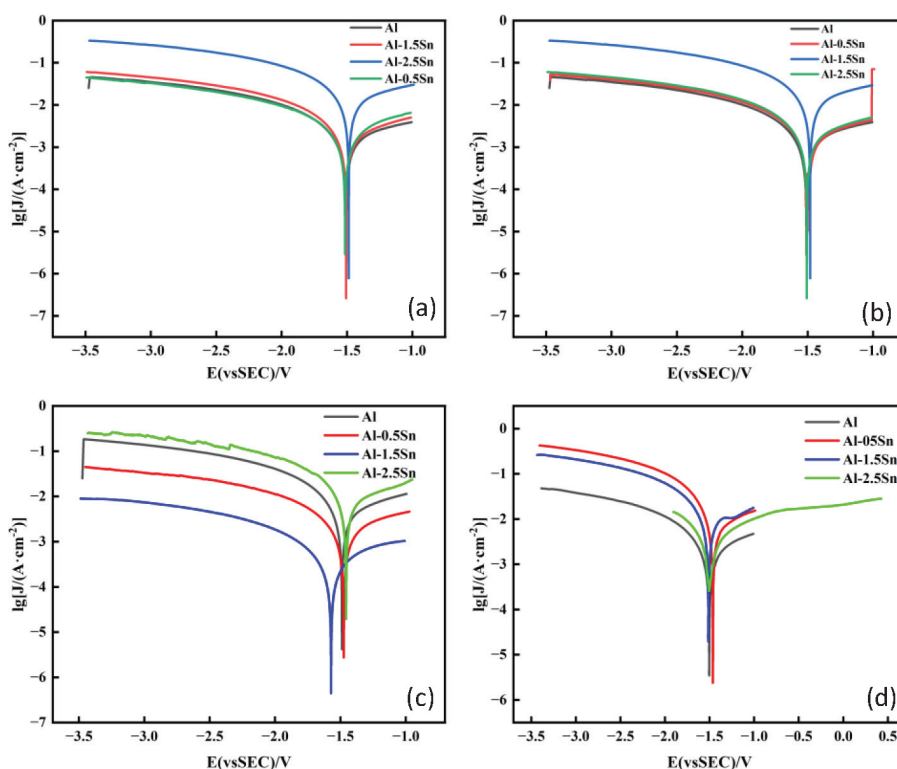


Figure 2: Potentiodynamic polarization curves of Al-Sn alloys subjected to different heat treatment temperatures: a) 480 °C, b) 490 °C, c) 500 °C, and d) control group (as-cast)

Consequently, the heat treatment fails to significantly improve the impedance characteristics of the Sn-modified aluminum alloys. Following heat treatment at 490 °C, the impedance behavior of the samples changes markedly. Pure aluminum still shows the highest impedance, while the Al-1.5Sn sample demonstrates relatively high impedance. In contrast, Al-0.5Sn and Al-2.5Sn exhibit lower impedance values. This indicates that 490 °C serves as a critical temperature, promoting the solid solution and redistribution of Sn in the aluminum matrix. The medium-Sn-content alloy benefits from improved microstructural homogeneity, leading to enhanced corrosion resistance. After heat treatment at 500 °C, the Al-2.5Sn sample exhibits the highest impedance, even surpassing that of pure aluminum. This demonstrates that high-temperature heat treatment significantly improves the electrochemical stability of high-Sn-content alloys. The elevated temperature facilitates uniform distribution of Sn and possibly leads to the formation of stable aluminum-tin compounds, effectively suppressing localized corrosion. The slight decrease in impedance observed for pure aluminum may be associated with grain growth, which reduces corrosion resistance.

This study employed a controlled experimental design to systematically investigate the synergistic mechanism of magnesium in tin-modified aluminum alloys. Using a gradient of Sn content (0.5 %, 1.5 %, 2.5 %) as the variable, control groups (Al-0.5Sn, Al-1.5Sn, Al-2.5Sn) and experimental groups (with corresponding 5 % Mg addition: Al-0.5Sn-5Mg, Al-1.5Sn-5Mg,

Al-2.5Sn-5Mg) were established. A comparative heat treatment was conducted at three solution temperatures, with all specimens undergoing 60-minute holding followed by water quenching and natural aging at room temperature for 72 h. To ensure variable uniqueness, the solution-treatment parameters were strictly consistent between Mg-containing and Mg-free alloys, with the Mg addition being the sole differentiating factor for the performance comparison. All specimens were finally processed into thin sheets measuring 0.8 mm × 0.8 mm × 1.0±0.05 mm to eliminate the influence of geometric dimensions on test results. **Figure 3-4** illustrates the open-circuit potential (OCP) variations of Al-Sn-Mg alloys after heat treatment, demonstrating that the addition of Mg effectively reduces the segregation of cathodic phases such as Sn through grain boundary pinning. After heat treatment at 490 °C, the OCP fluctuation range of the Al-1.5Sn-5Mg alloy decreased from ±10 mV (without Mg) to ±6 mV. A literature analysis suggests this phenomenon is likely attributed to the densification of the MgO/Al₂O₃ composite passive film. Typically, OCP fluctuations arise from the alternating activation and passivation processes of surface corrosion sites. Compared to Mg-free systems, Mg-containing alloys exhibit varying degrees of positive shifts in OCP, indicating a significant improvement in the thermodynamic stability of their passive films. In this experiment, the untreated Al-2.5Sn alloy displayed distinct trend-like OCP fluctuations, whereas the heat-treated samples primarily exhibited random fluctuations. This observation reflects nota-

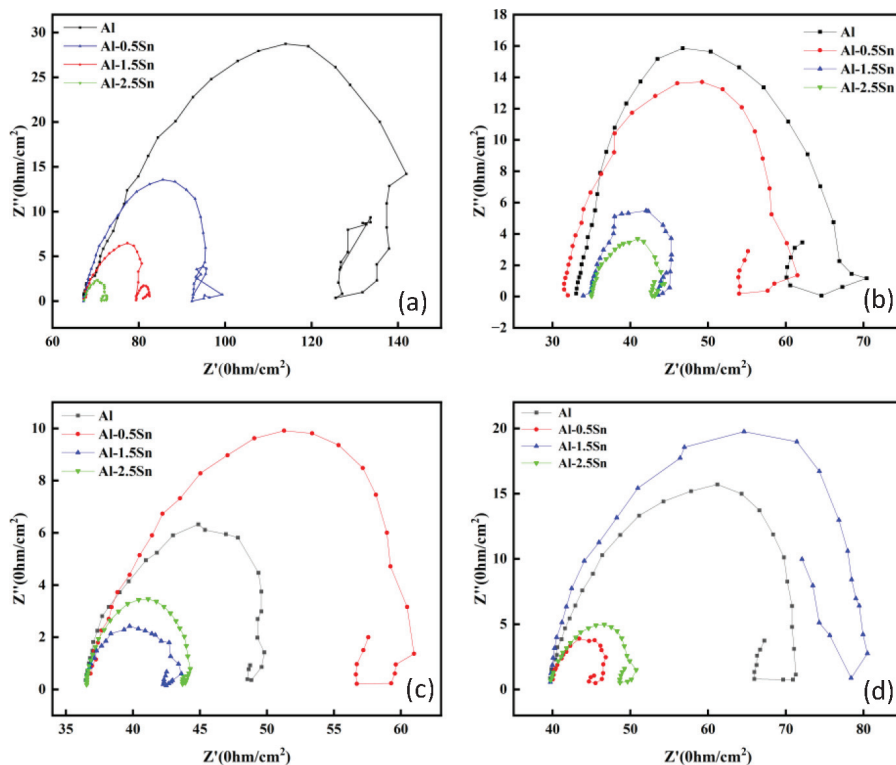


Figure 3: Electrochemical impedance spectra of Al-Sn alloys under different heat treatment temperatures: a) 480 °C, b) 490 °C, c) 500 °C and d) control group

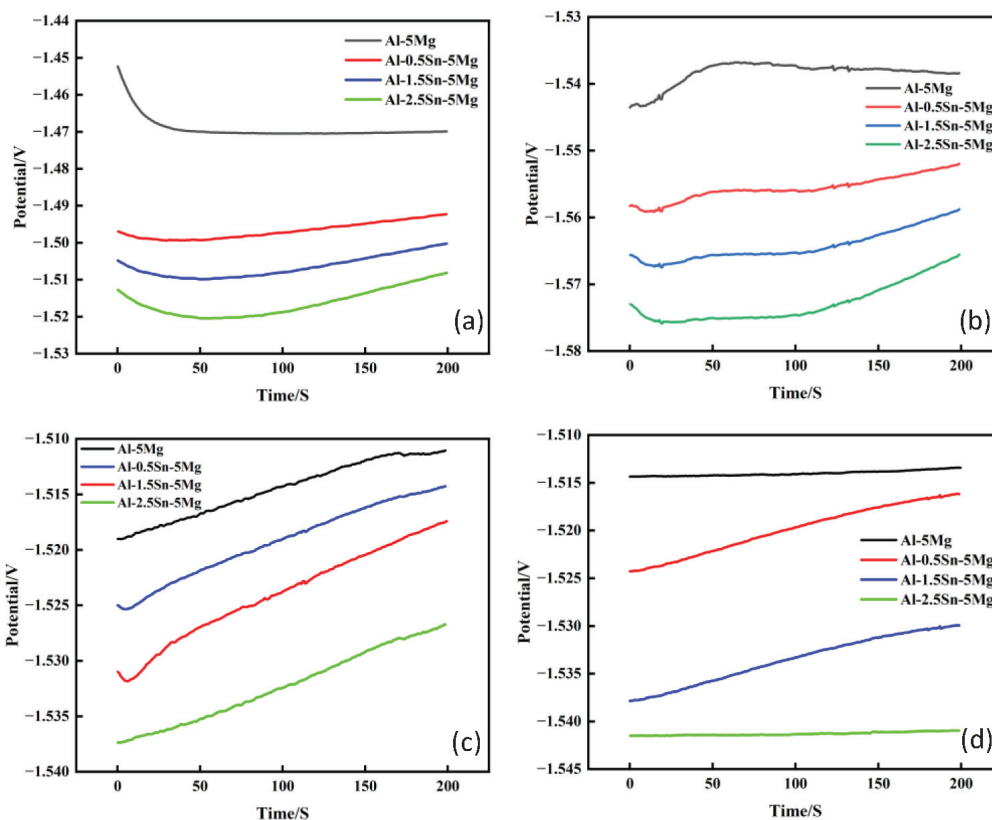


Figure 4: Open circuit potential of Al-Sn-Mg alloy at heat treatment temperatures: a) 480 °C, b) 490 °C, c) 500 °C, d) control group

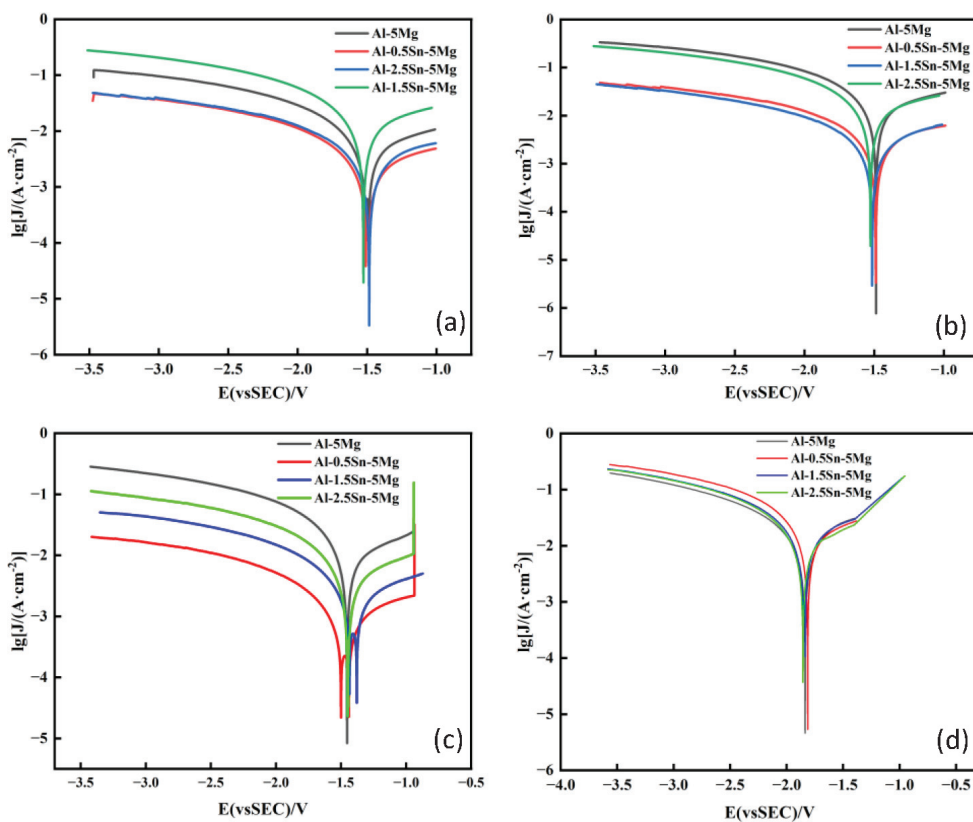


Figure 5: Potentiodynamic polarization curves of Al-Sn-Mg alloys under different heat treatment temperatures: a) 480 °C, b) 490 °C, c) 500 °C and d) control group

ble differences in the integrity of the passive films. Both Mg and Sn additions significantly influenced the hydrogen evolution behavior of the alloys: Mg promotes the hydrogen evolution reaction, leading to a negative shift in OCP, while Sn suppresses hydrogen evolution by increasing the hydrogen evolution overpotential. As the Sn content increases, the number and size of Sn-rich phases grow, enhancing their tendency to form micro-galvanic cells with the aluminum matrix and consequently inducing corresponding changes in OCP.

Analysis of the polarization curves for Al-Sn-Mg alloys after heat treatment (**Figure 5**) clearly demonstrates that the addition of 5 % Mg significantly alters the corrosion characteristics of the alloys. The incorporation of Mg promotes the formation of a protective Mg(OH)₂ layer, effectively enhancing the passivation behavior of the aluminum matrix. Specifically, all Mg-containing samples exhibit markedly superior corrosion resistance compared to their Mg-free counterparts, as evidenced by more positive corrosion potentials and lower corrosion current densities in the polarization curves. A notable synergistic effect is observed between Sn and Mg. Mg not only stabilizes the surface film but also mitigates the adverse effects of Sn content on corrosion performance. Polarization curve analysis confirms that both heat treatment and Mg addition are critical factors influencing corrosion behavior. Furthermore, samples subjected to heat treatment at 500 °C achieve optimal corrosion resistance, with Mg addition further enhancing this performance. The synergistic interaction between Sn and Mg

significantly improves the stability and protective quality of the surface layer, rendering these alloys particularly suitable for applications demanding a high corrosion resistance.

The Nyquist diagram in **Figure 6** illustrates the impedance characteristics of Al-5Mg and Al-Sn-Mg alloys in NaOH solution. The Al-5Mg alloy exhibits the largest impedance arc, indicating the best corrosion resistance among the tested samples. This high impedance suggests the formation of a stable and protective passive film on the Al-5Mg alloy surface, primarily attributed to the generation of MgO or Mg(OH)₂. The Nyquist diagram clearly demonstrates the influence of Sn content on the corrosion resistance of the alloys. The Al-5Mg alloy consistently shows the highest impedance arc, reflecting its excellent corrosion resistance, which is mainly due to Mg promoting the formation of a dense and stable passive film. In contrast, Sn-modified alloys exhibit lower impedance, with a significant decrease in corrosion resistance as Sn content increases. This reduction in impedance can be attributed to Sn disrupting the passive film and the potential for localized corrosion caused by the formation of Sn-rich phases. The electrochemical impedance behavior of Al-Sn-5Mg alloys with varying Sn content is shown in the diagram. The Al-5Mg alloy demonstrates the highest impedance, indicating the formation of a dense and stable passive film. Notably, the Al-0.5Sn-5Mg alloy shows significantly lower impedance than other Sn-containing alloys, suggesting weaker

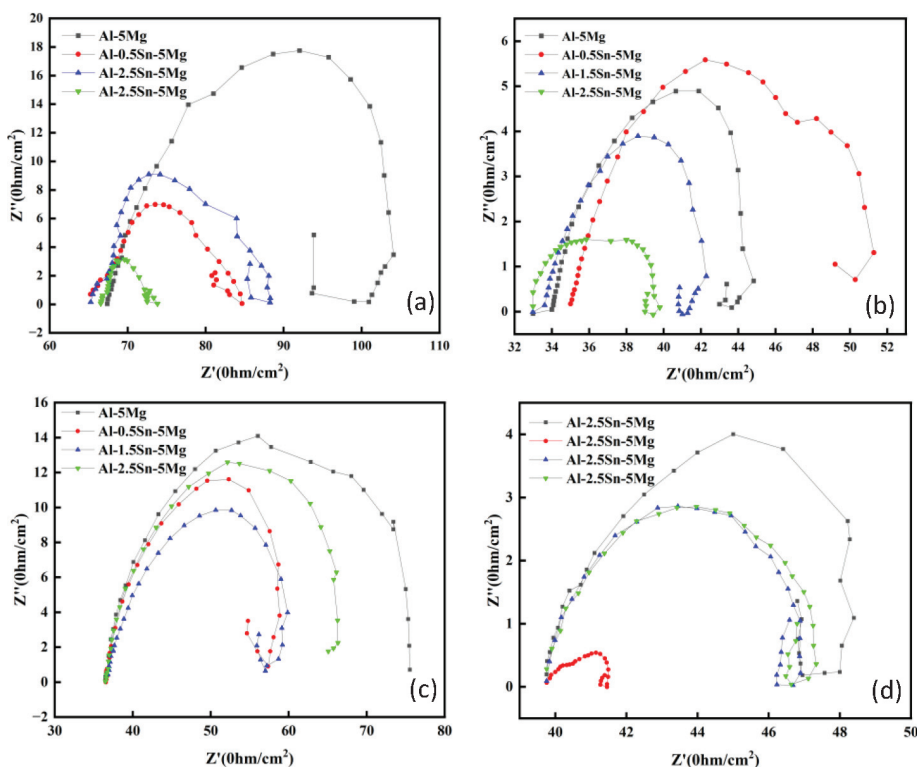


Figure6: Heat treatment temperature of aluminum-tin-magnesium alloy: a) 480 °C, b) 490 °C, c) 500 °C, d) impedance potential of the control group

protective properties of its passive film, likely due to insufficient Sn content leading to uneven distribution.

As the Sn content increases to 1.5 % and 2.5 %, the alloy impedance shows a slight enhancement. The higher Sn content may promote the formation of a more uniform passive layer, thereby partially mitigating its adverse effect on corrosion resistance.⁷

However, this improvement remains limited compared to the pure Al-5Mg alloy, highlighting the dominant role of the Mg in enhancing corrosion resistance. Among Sn-modified alloys, impedance initially decreases and then slightly increases with rising Sn content: the Al-0.5Sn-5Mg alloy shows the lowest impedance, associated with Sn disrupting the integrity of the passive film and inducing micro-galvanic corrosion. When Sn content further increases, impedance recovers slightly, indicating a potential stabilization effect under high Sn conditions. It is noteworthy that the Al-5Mg alloy maintains the highest impedance across all heat treatment temperatures, emphasizing the dominant role of Mg in enhancing passive film stability. In contrast, Sn-modified alloys generally exhibit lower impedance, with the Al-0.5Sn-5Mg sample being the most significantly affected by heat treatment. The combination of Sn and heat treatment may reduce passive film stability by promoting Sn segregation and forming less protective oxide layers.

Although this study did not directly quantify the change in cathodic phase area, the overall improvement in electrochemical performance suggests that the addition of 5 w/% Mg in the Al-Sn alloy similarly contributes to the improved performance, likely through analogous mechanisms such as "grain-boundary pinning" and "composite oxide-film formation."

A comparison with Mg-free alloys confirms that Mg addition significantly improves corrosion resistance. Mg-free alloys typically show lower impedance values, reflecting poorer protection from their passive films, while Mg promotes the formation of a denser and more stable oxide layer, effectively reducing corrosion rates. Although Sn serves as a modifying element, when combined with Mg under high concentrations or specific heat treatment conditions, it may instead weaken the protective properties of the passive film.

4 CONCLUSIONS

This study investigated the effects of heat treatment temperature and Mg addition on the electrochemical properties of Al-Sn alloys. The main findings are summarized as follows:

1. The effects of Sn and Mg dual modification and heat treatment on the electrochemical behavior of aluminum alloys in alkaline environments were investigated through electrochemical impedance spectroscopy and polarization curve analysis. The results indicate that heat treatment at 490–500 °C, near the maximum solid solubility of Sn (approximately 2.2 w/%), significantly im-

proves the alloy's performance, with 490 °C being the critical temperature for the Mg-free system. At this temperature, where the solid solubility of Sn approaches its peak, the Al-1.5Sn alloy exhibits optimal corrosion resistance: the corrosion current density is reduced by about one order of magnitude compared to the as-cast state, while the charge transfer resistance increases by nearly threefold. The high solid-solution Sn content suppresses grain boundary segregation and promotes the formation of a continuous Al₂O₃-SnO₂ composite passive film. Although excessive Sn can lead to grain boundary enrichment and exacerbate corrosion, treatment at 500 °C facilitates Sn diffusion and uniform distribution, enabling high-Sn alloys to achieve impedance performance superior to that of pure aluminum.

2. The addition of 5 % Mg proved instrumental in enhancing the corrosion resistance of the alloy. Electrochemical tests revealed that Mg exerts its beneficial effects through grain boundary pinning, which inhibits Sn segregation, and by promoting the formation of a dense MgO/Al₂O₃ composite passive film, creating a synergistic effect. In the Al-1.5Sn-5Mg alloy, this synergy manifests as exceptionally high electrochemical stability. Specifically, the open-circuit potential fluctuation of the alloy was reduced to within ±6 mV. Furthermore, its corrosion potential (*E*_{corr}) was shifted positively by more than 50 mV compared to a binary Al-1.5Sn alloy of similar composition, while the corrosion current density was reduced by an order of magnitude to approximately 2.5×10⁻⁷ A·cm⁻², indicating a significant decrease in the corrosion rate.

3. Under heat treatment at 500 °C, the synergistic interaction between Mg(OH)₂ and Sn resulted in the optimal performance of the Al-2.5Sn-5Mg alloy. Its Nyquist plot exhibited the largest capacitive arc diameter, and the fitted polarization resistance (*R*_p) was approximately 25 % higher than that of the Al-1.5Sn-5Mg alloy. This synergy effectively reversed the detrimental effect of high Sn content (2.5 w/%) typically observed in binary systems, restoring the impedance performance of the Mg-containing alloy to an excellent level. Through the coordinated regulation of microstructure and interfacial chemistry, Sn and Mg collectively enhanced the corrosion resistance of the alloy, thereby overcoming the limitations associated with single-element modification.

4. With a heat treatment at 490–500 °C and the introduction of 5 % Mg, the distribution of Sn and the characteristics of the passive film can be optimally controlled. In magnesium-free systems, Al-1.5Sn performs best, while in Mg-containing systems, Al-1.5Sn-5Mg and Al-2.5Sn-5Mg exhibit the most outstanding properties.

5 REFERENCES

- ¹ Wang C, Ning H, Liu S, et al. Enhanced ductility and strength of Mg-1Zn-1Sn-0.3Y-0.2Ca alloy achieved by novel micro-texture design. *Scripta Materialia*, 2021, 204: 114119

- ² Sasaki T T, Yamamoto K, Honma T, et al. A high-strength Mg-Sn-Zn-Al alloy extruded at low temperature. *J. Scripta Materialia*, 2008, 59(10): 1111-1114
- ³ Shen S, Yao S, Yang X, et al. Effect of Homogenization on Microstructure and Mechanical Properties of Al-Mg-Mn-Er Alloy. *J. Advanced Engineering Materials*, 2024, 26(8): 2302038
- ⁴ Hua Z-M, Wang C, Wang T-S, et al. Large hardening response mediated by room-temperature dynamic solute clustering behavior in a dilute Mg-Zn-Ca-Sn-Mn alloy. *J. Acta Materialia*, 2022, 240:118308
- ⁵ Xiao Z, Qiumei L, Donghui W, et al. Effect of aging process on fracture behavior of Al-0.55Mg-0.76 Si aluminum alloy. *J. WELDING & JOINING*, 2024 (8): 16-21
- ⁶ Wei S, Wang R, Zhang H, et al. Influence of Cu/Mg ratio on microstructure and mechanical properties of Al-Zn-Mg-Cu alloys. *J. Journal of Materials Science*, 2021, 56: 3472-3487
- ⁷ Li Z-G, Miao Y, Jia H-L, et al. Designing a low-alloyed Mg-Al-Sn-Ca alloy with high strength and extraordinary formability by regulating fine grains and unique texture. *J. Materials Science and Engineering: A*, 2022, 852: 143687
- ⁸ Chu J, Lin T, Wang G, et al. Effect of Heat Treatment on Microstructure and Properties of Al-7.0 Zn-1.5 Cu-1.5 Mg-0.1 Zr-0.1 Ce Alloy. *J. Metallography, Microstructure, and Analysis*, 2020, 9: 312-322
- ⁹ Martinez F, Junior C S, Leal J, et al. Effects of Sc Addition and Direct Aging Treatment on Microstructure and Hardness of AlSi10Mg Alloy. *J. Advanced Engineering Materials*, 2023, 25(19): 2300596
- ¹⁰ Wang Y, Wu R, Turakhodjaev N, et al. Microstructural evolution, precipitation behavior and mechanical properties of a novel Al-Zn-Mg-Cu-Li-Sc-Zr alloy. *J. Journal of Materials Research*, 2021, 36: 740-750
- ¹¹ Guo Z, Zhao G, Chen X G. Effects of homogenization treatment on recrystallization behavior of 7150 aluminum sheet during post-rolling annealing. *J. Materials Characterization*, 2016, 114: 79-87
- ¹² Yu L, Wang W, Wang J, et al. The effects of Sc addition on the microstructure and mechanical properties of Be-Al alloy fabricated by induction melting. *J. Journal of Materials Engineering and Performance*, 2019, 28: 2378-2387
- ¹³ Tang P, Pang R, Chen H, et al. Optimization of Microstructure and Mechanical Properties in Al-Zn-Mg-Cu Alloys Through Multiple Remelting and Heat Treatment Cycles. *J. Metals*, 2025, 15(3): 234
- ¹⁴ Zhang Z, Deng Y, Ye L, et al. Effect of multi-stage aging treatments on the precipitation and mechanical properties of Al-Zn-Mg alloys. *J. Materials Science and Engineering: A*, 2020, 785: 139394
- ¹⁵ Zhang C, Zhang Z, Liu M, et al. Effects of single- and multi-stage solid solution treatments on microstructure and properties of as-extruded AA7055 helical profile. *J. Transactions of Nonferrous Metals Society of China*, 2021, 31(7): 1885-1901
- ¹⁶ Wang Y F, Huang C X, Fang X T, et al. Hetero-deformation induced (HDI) hardening does not increase linearly with strain gradient. *J. Scripta Materialia*, 2020, 174: 19-23
- ¹⁷ Liu C Y, Zhang B, Ma Z Y, et al. Effect of Sc addition, friction stir processing, and T6 treatment on the damping and mechanical properties of 7055 Al alloy. *J. Journal of Alloys and Compounds*, 2019, 772: 775-781
- ¹⁸ Deng J, Shen J, Li H, et al. Investigation on microstructure, mechanical properties and corrosion behavior of Sc-contained Al-7075 alloys after solution-Aging treatment. *J. Materials Research Express*, 2020, 7(9): 096512
- ¹⁹ Li B, Wang X, Chen H, et al. Influence of heat treatment on the strength and fracture toughness of 7N01 aluminum alloy. *J. Journal of Alloys and Compounds*, 2016, 678: 160-166
- ²⁰ Zou Y, Wu X, Tang S, et al. Correlation between bulk and precipitate composition in Al-Zn-Mg-Cu alloys. *J. Philosophical Magazine Letters*, 2022, 102(2): 41-52